Volume 1 Nomor 3 October 2024
E-ISSN: 3047-4337

https://journal.antispublisher.com/index.php/IPTEKS/index

ENHANCING PVDF POLYMER PROPERTIES VIA VARIED BARIUM TITANATE MORPHOLOGIES AND SYNTHESIS TECHNIQUES: REVIEW

Haider Abdulelah 1, Zainab J. Sweah 2, Firas Fouad 3, Hussein Modhi 4
[1]Department of material science, polymer research center, university of Basrah, Iraq
[2]Department of Chemistry and polymer Tech., polymer research center, university of Basrah, Iraq
[3]Department of civil engineering, college of engineering, AL Muthanna university, Iraq
[4]Vocational Education, Iraq

Article Info

Article history:
Received Jun 10, 2024
Revised Aug 23, 2024
Accepted Sep 21, 2024

Keywords:
PVDF,
Barium Titanate,
Crystallinity,
Beta Phase,
Piezoelectric.

ABSTRACT

Background: Polyvinylidene fluoride (PVDF) is widely utilized in electronic devices due to its piezoelectric properties, which can be enhanced through the incorporation of barium titanate (BT). However, the impact of various fabrication methods on the crystallinity and beta-phase content of PVDF/BT nanocomposites remains underexplored. **Specific Background**: Different manufacturing techniques, including 3D printing, electrospinning, solvent casting, and compression molding, influence the structural and functional properties of PVDF/BT composites. The crystallinity and beta-phase content of PVDF are critical for optimizing the dielectric and piezoelectric performance of these materials. **Knowledge Gap**: There is a lack of comprehensive studies comparing the effects of these fabrication techniques on the crystallinity and beta-phase enhancement of PVDF/BT composites, particularly concerning their dielectric, piezoelectric, and mechanical properties. **Aims**: This study aimed to investigate the impact of integrating BT into PVDF using various fabrication methods on the crystallinity and beta-phase formation. The goal was to determine how these modifications influence the material's structural characteristics and, consequently, its electronic properties. **Results**: X-ray Diffraction (XRD) and Fourier-Transform Infrared Spectroscopy (FTIR) analyses revealed that 3D printing and electrospinning methods significantly enhanced the beta-phase content and crystallinity of PVDF/BT composites compared to solvent casting and compression molding. Scanning Electron Microscopy (SEM) confirmed improved morphological features in the PVDF matrix with these techniques. **Novelty**: This study provides new insights into how different fabrication methods can optimize the crystallinity and beta-phase of PVDF/BT nanocomposites, which are crucial for enhancing piezoelectric performance. **Implications**: The findings suggest that 3D printing and electrospinning are superior to traditional methods for fabricating PVDF/BT composites with enhanced piezoelectric properties. These results can guide the development of more efficient electronic devices by selecting appropriate fabrication techniques to achieve desired material properties.

Corresponding Author:
Haider Abdulelah
University of Basrah
E-mail address: haider.abdulelah@uobasrah.edu.iq
DOI : https://doi.org/10.61796/ipteks.v1i3.183

INTRODUCTION

Polyvinylidene fluoride (PVDF) is a versatile polymer that has gained significant attention in materials science and technology due to its unique combination of piezoelectricity, chemical stability, and mechanical robustness. PVDF has high dielectric constant and good electroactive make it suitable for advanced sensing and energy storage systems [1]. Recent advancements in PVDF-based nanocomposites include the introduction of barium titanate nanostructures to enhance the piezoelectric performance and high-capacitance dielectric materials for capacitor applications [2,3]. These nanocomposites have been prepared using various methods such as solution-cast method [4], hot-press blending, non-isothermal crystallization, coating, and annealing [5]. The addition of BT in the PVDF matrix has been found to alter the crystallinity and morphology of the PVDF polymorphs [6]. The addition of BT nanoparticles to PVDF enhances the dielectric and ferroelectric properties of the nanocomposites, resulting in improved energy density and polarization [7]. The crystallization of PVDF is influenced by factors such as molecular order, diffusion coefficient, crystal growth rate, and external deformation. The molecular weight of the amorphous component in PVDF blends affects the diffusion coefficient and crystal growth rate of the crystalline component [8-11]. Several researchers investigated the shapes of various nanofillers and their effects on PVDF crystallization exclusively in the alpha phase and the β-phase [12-16]. Lin et al. achieved a notable 90.2% β-phase crystal structure in PVDF composite films with BaTiO3 and MWCNT, attributing the success to their combined impact. [17]. Caifeng et al. detailed the fabrication of electroactive PVDF thin films through a 3D printing process, optimizing parameters to enhance β-phase and crystallinity. [18]. The primary objective of this study is to offer mechanistic insights into the intricate processes of nucleation and growth. It focuses on improving crystallization in polyvinyl fluoride by adding barium titanate, considering specific factors during manufacturing. Furthermore, the research includes selecting an optimal manufacturing method for the composite material to enhance crystallization and, consequently, improve piezoelectric applications.

METHODS

The study highlights the crucial role of the synthesis method in determining the crystalline properties of barium titanate, emphasizing its malleability. Various synthesis approaches introduce variations in crystal structure, grain size, and defects, collectively influencing the overall crystallinity of material.

2.1. Solid-State Reaction

Barium titanate powder synthesis involved a 1:1 ratio of barium carbonate (99% purity) and titanium dioxide (99.9% purity). Equimolar BaCO3 and TiO2 powders were mixed in acetone, dried at 60°C, and calcined at 900°C for 3 hours. The resulting powder underwent low-temperature solid-state synthesis with added BaTiO3 seeds to enhance crystallinity [19].

2.2. Sol-Gel Method

Barium titanate was synthesized via the sol-gel method using barium acetate and titanium tetra iso-propoxide. The components were dissolved separately in 2-methoxy ethanol, combined, and stirred to form a sol. The sol was exposed to an infrared lamp, resulting in a gel dried at 80°C and annealed at 650°C for 2 hours to produce barium titanate powder [20].

2.3. Hydrothermal Synthesis

BaTiO3 was synthesized through a precipitation-aging method with BaCl2 2H2O, TiCl4 solution, and NaOH. Adjusting slurry volume with deionized water or ethylene glycol, hydrothermal treatment produced tetragonal BaTiO3 rods with 10 vol% EG [21].

2.4. Mechanochemical Synthesis

A uniform BaTiO3 structure was achieved through mechanochemical processing in a high-energy planetary ball mill. The oxides underwent initial heat treatment, followed by milling for 1.5 hours at room temperature [22,23].

2.5. Microwave-Assisted Synthesis

Tetragonal-phase BaTiO3 powders were synthesized using microwave sintering at 850°C. BaCO3, TiO2, and alanine served as raw materials, with Sic microspheres acting as microwave conductors to facilitate uniform heating and reduce calcination temperature [24].

Table 1 presents a comparative analysis of how different synthesis methods impact the crystalline structure of barium titanate, revealing insights into homogeneous crystal growth, enhanced size, irregular morphology, rapid crystallization, and homogeneous crystal growth induced by various manufacturing techniques.

Table 1: Effect of Various synthesis Methods on the Crystalline Structure of Barium Titanate

No.	synthesis Method	Effect on Structure	Ref.
1.	Sol-Gel Method	Achieves a homogeneous crystalline structure	[25]
2.	Hydrothermal Synthesis	Enhances crystal size & Yields a high degree of crystallinity	[26,27]
3.	Solid-State Reaction	Results in irregular crystalline morphology	[28]
4.	Microwave-Assisted	Induces a rapid crystallization process	[29]
5.	mechanochemical Synthesis	Promotes homogeneous crystal growth	[30]

3. Preparation of PVDF/Barium Titanate Nanocomposites

Diverse approaches are employed in the preparation of PVDF/Barium Titanate (PVDF/BT) nanocomposites, each offering distinct advantages and implications for the resulting structural characteristics. Prominent techniques include solution blending, melt mixing, and in situ polymerization.

Table 2: Effect of Synthesis Methods on Structural Properties of PVDF Nanocomposites

Synthesis Method	Influence on Structural Properties	Ref.
Solution Blending	Better dispersion and compatibility due to the dissolution process, resulting in improved interfacial interaction.	[31]
Melt Mixing	Simplicity, but may lead to uneven distribution and agglomeration, affecting overall homogeneity.	[32]
In situ-Polymerization	Precise control over nanocomposite structure, influencing crystallinity, particle size, and morphology. Potential to enhance piezoelectricity and mechanical strength	[33,34]

4. Fabrication of PVDF/Barium Titanate Nanocomposites

Various fabrication methods, including 3D printing, electrospinning, compression molding, and solvent casting, significantly influence the crystalline and phase properties of PVDF nanocomposites. These methods, such as 3D printing, provide precise spatial control for intricate designs but have constraints in material selection and potential degradation. Electrospinning enhances mechanical and electrical properties through nanofiber production but faces challenges in scalability and versatility. Compression molding ensures efficient production and consistent properties for large-scale applications, although it has limitations in part complexity and higher equipment costs.

Solvent casting, cost-effective and versatile, presents challenges like limited spatial control, material degradation, and optimization difficulties, especially in achieving uniformity in crystalline and phase characteristics in PVDF and its nanocomposites [35-38].

5. Characterization for the identification of crystallinity

X-ray Diffraction (XRD) analysis serves as a potent tool for examining the crystalline structures of Polyvinylidene fluoride (PVDF)/Barium Titanate (BT) nanocomposites. It provides valuable insights into the influence of BT concentrations on crystallinity, crystallographic structures, and phase transitions within the composite material. Fourier-Transform Infrared Spectroscopy (FTIR) is a powerful technique for unraveling molecular interactions in PVDF/BT nanocomposites, particularly at their interface. SEM plays a crucial role in characterizing nanocomposites across various fabrication processes, offering detailed morphological information and surface topography analysis indispensable for assessing quality and properties. Additionally, DSC analysis contributes to understanding crystallization growth.

RESULT AND DISSCUSION

6.1. X-ray Diffraction (XRD) Analysis

Table 3 aims to provide a concise overview of fabrication methods and their impact on crystallinity in materials. It summarizes key findings regarding the relationship between fabrication methods and crystallinity in XRD analysis across different studies. The examined fabrication methods include Compression Molding, 3D Printing, and Electrospinning, with each study emphasizing specific effects on crystallinity.

Table 3: Summary of XRD Analyses in PVDF/BT Nanocomposites

Study	Fabrication Method	Crystallinity in XRD Analysis Effect
Brunengo et al. (2018) [39]	Compression Molding	1) Increased crystallinity under pressure and temperature. 2) Possible crystalline orientation along the molding axis. 3) Enhanced compatibility between PVDF and Barium titanate.
Song et al. (2021)[40]	3D printing	1) Layered structure may cause varied crystallinity along layers. 2) Peak broadening due to potential amorphous phases. 3) Crystalline orientation influenced by printing parameters.
Kumar. et al. (2021) [41]	Electrospinning	1) Increased crystallinity from nanoscale fiber formation. 2) Enhanced surface area promotes crystalline growth.

	3) Possible crystallite orientation along electrospun fibers.

6.2. Fourier-Transform Infrared Spectroscopy (FTIR)

Table 4 summarizes the impact of fabrication techniques on FTIR spectra, providing insights into molecular and structural changes. The concise overview includes well-defined crystalline peaks and molecular alterations observed in Compression Molding, 3D Printing, and Electrospinning.

Table 4: Overview of FTIR Analyses in PVDF/BT Nanocomposites

Study	Fabrication Method	Crystallinity in FTIR Spectra Effect
Olmos et al. (2013) [42]	Compression Molding	1) Well-defined peaks for crystalline PVDF phases. 2) Shifts or intensity changes signaling molecular alterations. 3) Presence of characteristic peaks for PVDF and Barium titanate. 4) Broadening or splitting of peaks from compression effects.
Kaur, G et al. (2020) [43]	3D Printing	1) Potential variations in peak shapes and intensities. 2) Distinctive features in interlayer regions from the printing process. 3) Peaks related to amorphous phases present between printed layers. 4) Crystalline peaks shift based on printing parameters.
Ramasundaram et al. (2019) [44]	Electrospinning	1) Enhanced crystallinity demonstrated by sharp and defined peaks. 2) Presence of additional peaks due to interactions in nanofiber matrix. 3) Crystalline orientation along electrospun fibers may be observed. 4) Absorption bands corresponding to PVDF and Barium titanate.

6.3. Scanning Electron Microscopy (SEM)

Table 5 outlines the Advantages and Challenges of Compression Molding, 3D Printing, and Electrospinning. It highlights advantages such as high-resolution surface analysis, layer-by-layer examination, and nanofiber morphology characterization. Challenges encompass sample preparation precision, resolution limitations in complex structures, and potential charging effects.

Table 5: Summary of Advantages and Challenges in Various Fabrication Processes for SEM Results in PVDF/BT Nanocomposites.

Fabrication Process	**Compression Molding [45]**	**3D Printing [46]**	**Electrospinning [47]**
Advantages	High resolution: SEM provides detailed surface analysis.	Layer-by-layer analysis: SEM examines individual layers.	Nanofiber characterization: SEM studies nanofiber morphology.
	Morphological characterization: Reveals BT distribution in PVDF matrix.	Surface quality assessment: SEM helps evaluate printing quality.	- Fiber alignment: SEM reveals nanofiber alignment.
	Surface topography: Examines surface roughness and uniformity.	- Surface topography: SEM assesses surface roughness and quality of each layer.	- Surface topography: SEM examines nanofiber surface roughness and uniformity.
Challenges	Sample preparation: Crucial for accurate imaging, requires care.	Resolution limitations: Achieving high resolution in complex structures is challenging.	Charging effects: Electro-spun samples may exhibit SEM charging effects.
	Limited depth information: SEM primarily provides surface information.	Post-processing effects: Some steps may alter surface characteristics.	Sample preparation: Similar to compression molding, proper preparation is crucial.

Table 6 summarizes the impact of Barium Titanate (BT) processing methods on crystallinity and SEM observations. Compression Molding, 3D Printing, and Electrospinning with BT nanoparticles and Nanorods/Nanowires showcase unique characteristics such as uniform dispersion, layer-by-layer construction, and fibrous structure, respectively.

Table 6: Crystalline effects by Processing Techniques and BT Morphologies

Processing Method	**BT Shapes**	**Crystalline influences**	**Observations in SEM Images**
Compression Molding	BT Nanoparticles	Moderate crystallinity increases from uniform dispersion.	BT nanoparticles disperse in PVDF, enhancing structure [48].
	BT Nanorods/Nanowires	Significant crystallinity increases with directional alignment.	BT shapes align, influence properties. SEM captures nanorods/nanowires [49,50]
3D Printing	BT Nanoparticles	Moderate increase with layered construction and uniform dispersion.	SEM displays layered BT construction for homogeneity. [51]
	BT Nanorods/Nanowires	Moderate increase with layer alignment. Enhanced crystallinity in nanowire layers.	Elongated shapes impact interlayer adhesion. SEM details nanorods or nanowires in each layer [52,53]
Electrospinning	BT Nanoparticles	Moderate increase due to uniform dispersion in fibrous structure.	Uniform nanofiber distribution influences properties [54]
	BT Nanorods/Nanowires	Enhanced crystallinity with aligned nanorods or nanowires in fibrous structure.	Elongated structures align along nanofibers. [55,56]

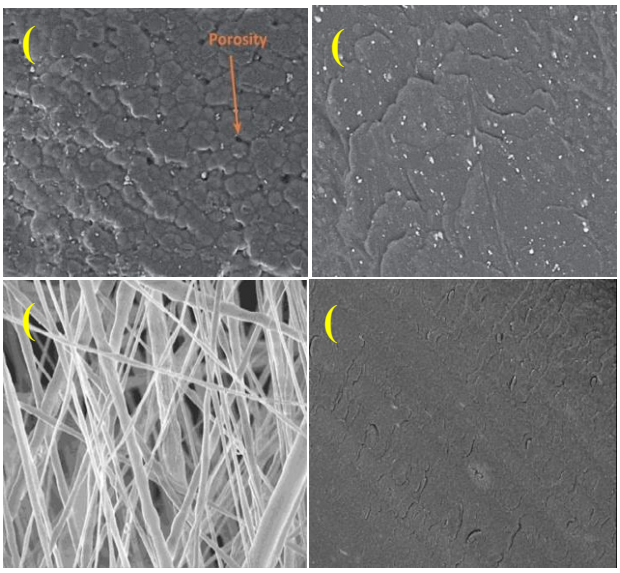

Figure 1: Illustrate the morphology of different fabrication processes of PVDF nanocomposites, (a) solvent-casted, (b) 3D printing, (c) Electrospinning, (d) Compression molding [58,51,57].

5.4. Effect of Filler Content and Filler Size on Crystallinity, Phase Content, and Properties

In the PVDF/DMF solution, dipolar interactions and hydrogen bonding disrupt polymer chains, influencing the crystallization process. BaTiO3 nanoparticles serve as nucleating agents, fostering hydrogen bonds and a characteristic TTT configuration in the β-phase of PVDF. Figure 2(a) illustrates O – H stretch hydrogen bonds. Both nanoparticle size and chemical structure play crucial roles in nucleating the electroactive β-PVDF phase in melt-processed composites. In Figure 2(b) and (c), infrared spectra of α- and β-PVDF reveal the prevalence of the β-phase through an absorption band at 840 cm-1. Calculations based on absorption bands at 764 and 840 cm-1 demonstrate the pivotal role of BaTiO3 nanoparticles in promoting crystallization of the electroactive β-phase within the PVDF matrix.

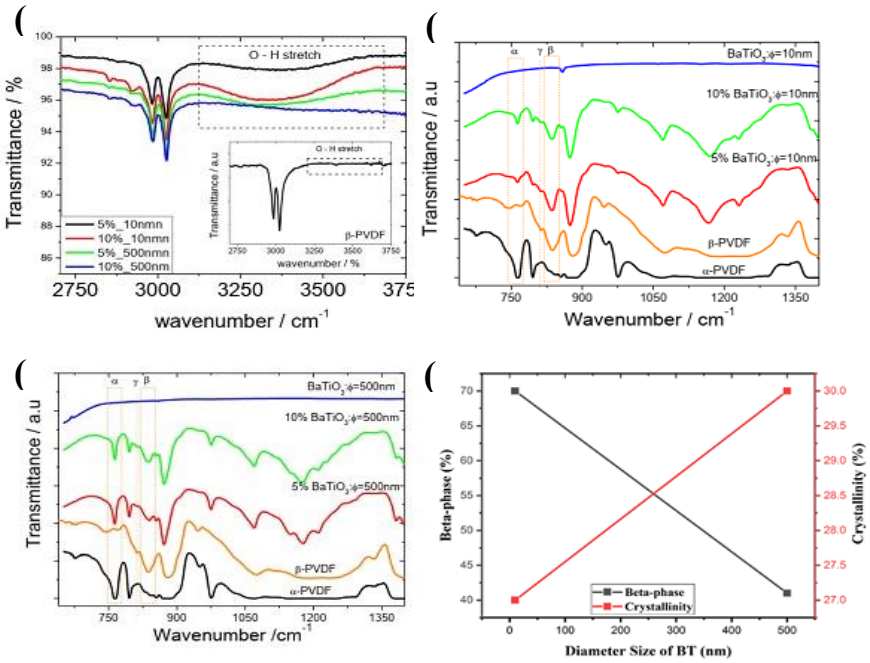

Figure 2: displays FTIR spectra: (a) the PVDF/BaTiO3 composites and the pure polymer (inset) in the O – H region, (b) PVDF/BaTiO3 samples with varied filler contents at average filler sizes of 10 nm, and (c) at 500 nm, (d) illustrates correlations between diameter size and beta phase as well as crystallinity[59].

The calculation of β-phase crystallization content (F(β)) is performed using Eq. (1).

$$F(\beta) = I_\beta/(1.26 * I_\alpha + I_\beta)$$

Where, I_α & I_β the absorbed intensity of alpha phase and beta phase, respectively. Notably, the highest electroactive phase content (F(β) = 82%) is achieved with the smallest Barium titanate nanoparticle concentration and average size (D = 10 nm), emphasizing the impact of particle characteristics on the nucleation process. To quantify the degree of crystallinity (X_c) of these samples, an evaluative approach involved numerical determination by calculating the ratio of crystalline peak areas to the total area generated from these peaks, as depicted in the following equation:

$$X_c = A_c/(A_c + A_a) \quad (2)$$

where, A_c is the total integrated area under the XRD peaks and $A_c + A_a$ are the integrated intensities corresponding to the crystalline and amorphous phases, respectively.

In Figure 3(a,b), the SEM image reveals the microstructure of PVDF/BaTiO3 composites with consistent features at 500nm filler sizes and 10% filler concentrations. The spherulitic structure, with small pores between spherulites, indicates the growth and expansion of crystalline structures during solidification. As crystallization progresses, voids form between crystallized spherulites, denoting the absence of a liquid phase (Figure 3a). The nanocomposite microstructure closely resembles that of neat α-PVDF, featuring spherulites with concentric rings, while neat β-PVDF displays smaller, porous spherulites, indicating comparatively inferior mechanical and electrical properties. Backscattering images further demonstrate a well-distributed dispersion of nanofillers, emphasizing uniformity in the composite structure (Figure 3b). Figure 3(c,d) highlights the impact of filler size and concentration on β-phase composition in PVDF/BaTiO3 composites. At 5% filler content, the 10nm filler shows 82% β-phase, while the 500nm filler exhibits 42%. Increasing filler content to 10%, the 10nm filler has 70% β-phase, and the 500nm filler has 41%. On other hand, an increase in filler concentration leads to a general decrease in β-phase content for both filler sizes. In Figure 3(d), at 5% BaTiO3 content, the 500nm filler demonstrates higher crystallinity (36%) than the 10nm filler (33%). At 10% BaTiO3 content, both fillers show reduced crystallinity, with the 10nm filler at 27% and the 500nm filler at 30%. These findings emphasize the influence of filler size and content on β-phase composition and crystallinity in PVDF/BaTiO3 nanocomposites, highlighting their significant role in material properties

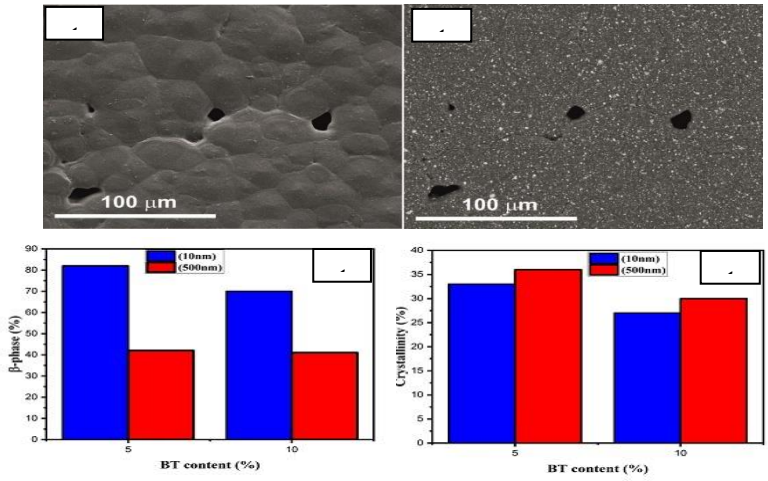

Figure 3: a) SEM Image of PVDF/BaTiO3 Composites with 10% Filler Concentration and 500 nm Filler Size b) Corresponding backscattering image, c) Correlation between Concentration and Beta Phase for Different Diameter Sizes, and, d) Correlation between Concentration and Crystallinity for Different Diameter Sizes.

Figure 4 demonstrate that the storage modulus, dielectric constant, and permittivity of PVDF/BaTiO3 composites are strongly influenced by both the BT content and filler size. In Figure 4(a), BT content (0%, 5%, 10%) is correlated with storage modulus values for composites featuring different filler sizes (10nm and 500nm). The

10nm filler consistently shows higher storage modulus values compared to the 500nm filler, especially at higher BT content. At 5% BT content, the 10nm filler exhibits a significant increase to 2250 MPa, while the 500nm filler reaches 1250 MPa. With 10% BT content, the storage modulus further increases to 2350 MPa for the 10nm filler, while the 500nm filler shows a decrease to 4 MPa. In Figure 4(b), the rise in dielectric constant is linked to an increase in the dissipation factor, which generally increases with higher filler size and content. Figure 4(c) At pure PVDF exhibit a permittivity of 12. With 5% BT content, the 10nm filler size significantly increases to 35, while the 500nm filler exhibits value 14. At 10% BT content, the permittivity further rises to 57.5 for the 10nm filler and 22 for the 500nm filler. The increase in dielectric constant and permittivity with increasing BT content is more pronounced for the 10nm filler size, indicating a greater sensitivity to BT content changes.

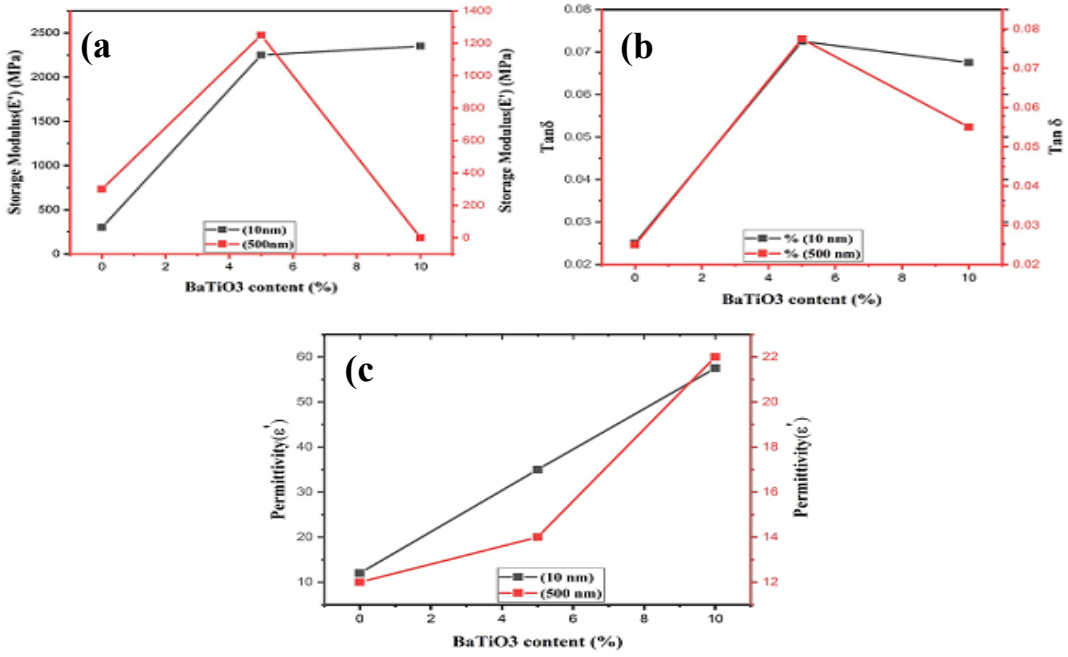

Figure 4 illustrates the relationship between BaTiO3 content and the (a) storage modulus, (b) dissipation factor, and (c) permittivity at various diameter sizes

Figure 5 illustrates the influence of BaTiO3 content on Mechanical, Thermal, and Dielectric Characteristics of PVDF nanocomposite. At pure PVDF, the polymer displays an 81% β-phase content, Tensile Strength of 100 MPa, Tensile Modulus of 1.5 GPa, and Glass Transition Temperature (Tg) of -37.33°C. With a 10% BaTiO3 content, the β-phase content increases to 84%, enhancing mechanical properties with a Tensile Strength of 140 MPa and Tensile Modulus of 1.7 GPa. However, Tg and tan δ show slight decreases. Further increases to 20% and 40% BaTiO3 result in higher β-phase content (87% at 40%),

improving Tensile Strength and Modulus. Notably, Relative Permittivity rises significantly, peaking at 40%, while Tg decreases. The increase in β-phase content positively correlates with improved mechanical strength, but the decrease in Glass Transition Temperature suggests changes in the polymer's thermal behavior. The significant rise in Relative Permittivity at higher BaTiO3 contents indicates enhanced dielectric properties, valuable for certain applications[60].

Figure 5. (a) Correlation between beta phase and BaTiO3 content, (b) Effect of BaTiO3

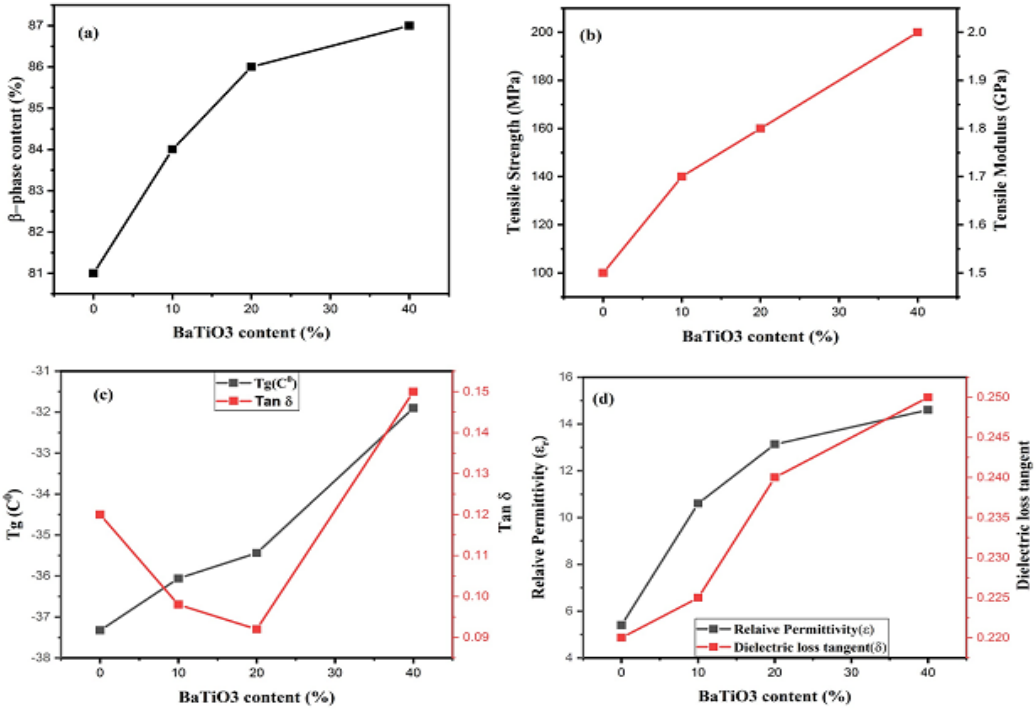

Content on Properties of PVDF Composites: Mechanical, Thermal, and Dielectric Characteristics.

5.5. Effect of fabrication methods on Crystallinity, Phase Content, and Properties

The observed trends in the results highlight the significant influence of fabrication methods on the crystallinity and beta-phase composition of PVDF/BaTiO3 composites. Three-dimensional printing and electrospinning consistently demonstrate superior outcomes with higher beta-phase values (4.6% and 3.7%, respectively) and moderate crystallinity compared to compression molding and solvent casting. The inferior performance of solvent casting is attributed to its limited impact on the alignment of BaTiO3 within the PVDF matrix, resulting in lower crystallinity and beta-phase values. The negative beta-phase and crystallinity values in solvent-casted samples, particularly -25% for beta-phase, raise concerns about the absence of desired nanocomposite characteristics. These findings emphasize the crucial role of fabrication methods in

tailoring the material properties, urging a careful consideration of manufacturing techniques for optimal performance in PVDF/BaTiO3 composites [61,58,62,63].

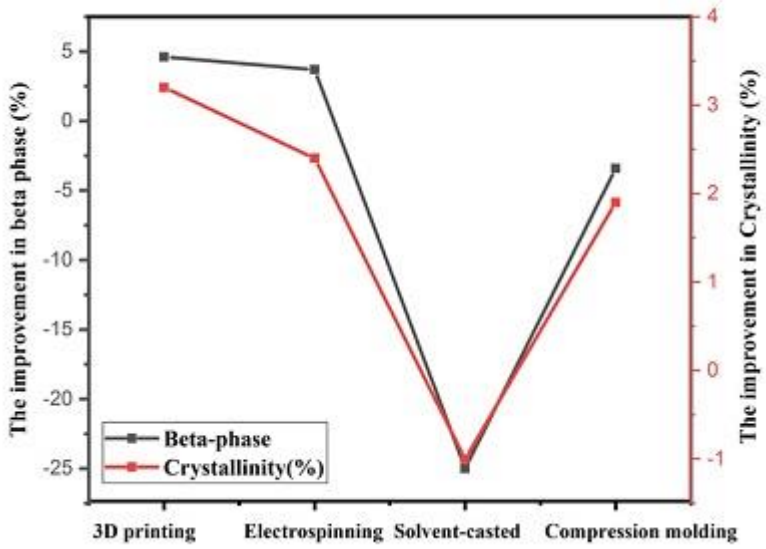

Figure 6: Effect of Fabrication Methods on Crystallinity and Beta Phase

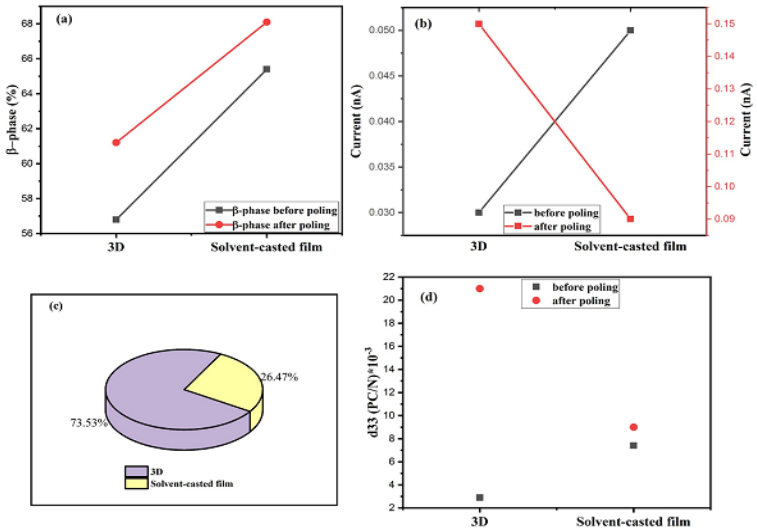

Figure 7 presents a comparative analysis of beta-phase, current, and d33 values in PVDF composites manufactured through 3D printing and solvent-casting film processes, both pre and post-poling.

In 3D-printed composites, beta-phase increases from 56.8% to 61.2%, accompanied by a substantial improvement in current from 0.03 to 0.15, resulting in a noteworthy d33 increase from 2.9 to 21. Conversely, solvent-casted film PVDF composites show enhanced beta-phase from 65.4% to 68.1% post-poling, despite a slight current decrease from 0.05 to 0.09. The d33 value experiences a positive shift from 7.4

to 9. Overall, results underscore the efficacy of both 3D printing and solvent-casting in enhancing beta-phase and electrical properties in PVDF composites post-poling [64].

Figure 7: (a) Comparison of Beta Phase Content between 3D and Solvent-Casted Manufacturing Methods with or without Poling, (b) Comparison of Current Output between 3D and Solvent-Casted Manufacturing Methods with or without Poling, (c) PE Diagram Illustrating Improvement Percentage in Output between the Two Methods, (d) Comparison of Piezoelectric Coefficient between the Two Methods.

A substantial rise in current (26.4(solvent casted) % to 73.53% (3D printing)) signifies enhanced charge transport, crucial for superior electrical conductivity in piezoelectric materials. The layer-by-layer additive manufacturing process in 3D printing enables precise microstructure control, minimizing defects and resulting in superior piezoelectric properties in PVDF nanocomposites. Figure 8 outlines the influence of BaTiO3 content on various properties of the composite material. As BaTiO3 content increases from 0% to 50%, density rises from 1.7 to 2.6 g/cm³, reflecting the increasing concentration of the filler. Microhardness also shows an upward trend, reaching 7.3 kg/mm² at 0% and 9.7 kg/mm² at 50%. The dielectric constant at 1KHz varies from 8.7 (0% filler) to 31.3 (50% filler), while at 1MHz, it ranges from 7.25 to 22.6. Additionally, the Dissipation Factor increases with filler content, peaking at 0.16 for 50% filler [65].

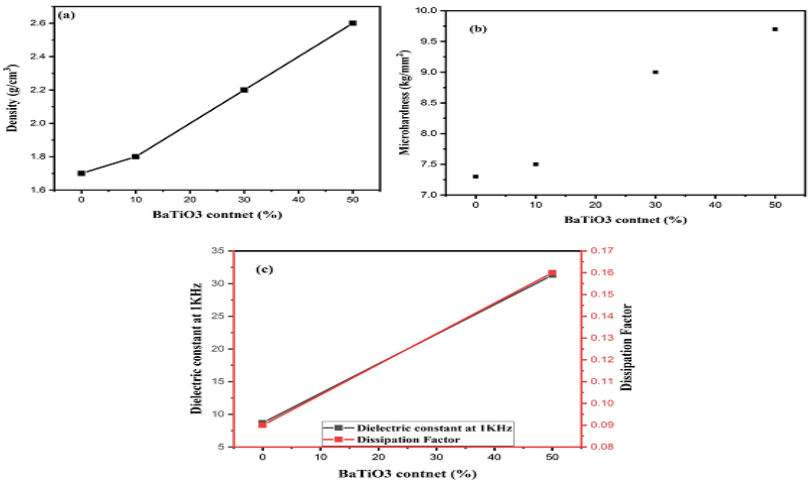

Figure 8 illustrates the impact of BaTiO3 content on (a) density, (b) microhardness, and (c) dielectric constant.

These findings highlight the significant impact of BaTiO3 content on the composite's density, mechanical strength, and dielectric properties, crucial for applications in diverse fields. Figure 9 displays SEM images of electro-spun PVDF/BaTiO3 nanocomposites at 10,000x magnification. The enhanced performance is attributed to morphological changes post-electrospinning, where the electric field-

induced polarization aligns dipole moments in PVDF chains and BaTiO3 nanoparticles. Specifically, in variant A (5% PVDF/BaTiO3), PVDF), BaTiO3 nanoparticles exhibit a linear and uniform distribution within PVDF nanofibers, ensuring efficient charge transmission during mechanical vibrations. Conversely, variant B(10%PVDF/BaTiO3) with non-uniform distribution, leads to reduced dipole moments and diminished charge transfer, resulting in lower piezoelectric output. In variant C(15%PVDF/BaTiO3), a micro-beaded structure, coupled with uneven distribution, further hampers dipole moment alignment and charge transfer, yielding reduced performance compared to pure PVDF. The optimal power output, at 1.56 V, is achieved by variant A, showcasing superior piezoelectric energy harvesting with a power output of 0.243 μW and a power output density of 0.02 μW/cm2. In Figure 10, the intricate interplay between Barium Titanate content, fiber diameter, beta phase percentages, tensile properties and voltage output is highlighted. Figure 10(a) and (b) specifically examine the effects of Barium Titanate content and fiber diameter on beta phase percentages and voltage values, respectively. For instance, at 5% Barium Titanate content, a fiber diameter of 554.3 is associated with an 83% beta phase and a voltage of 2. Increasing Barium Titanate content to 10% while maintaining a constant fiber diameter of 672.2 nm results in an 82% beta phase and a reduced voltage of 1.5. Conversely, at 15% Barium Titanate content with a fiber diameter of 453 nm, the beta phase slightly decreases to 81%, and the voltage further reduces to 1.2. Figure 10(c), the tensile strength and elongation properties of PVDF and PVDF/15BT composites are presented. The PVDF sample exhibits a tensile strength of 45.83% and an elongation of 50%. On the other hand, the PVDF/15BT composite shows a tensile strength of 7.63% and an elongation of 550%. These results indicate a significant impact on the mechanical properties with the addition of 15% Barium Titanate (BT) to the PVDF matrix. The reduced tensile strength and increased elongation suggest changes in material behavior, which could be attributed to the incorporation of Barium Titanate [66].

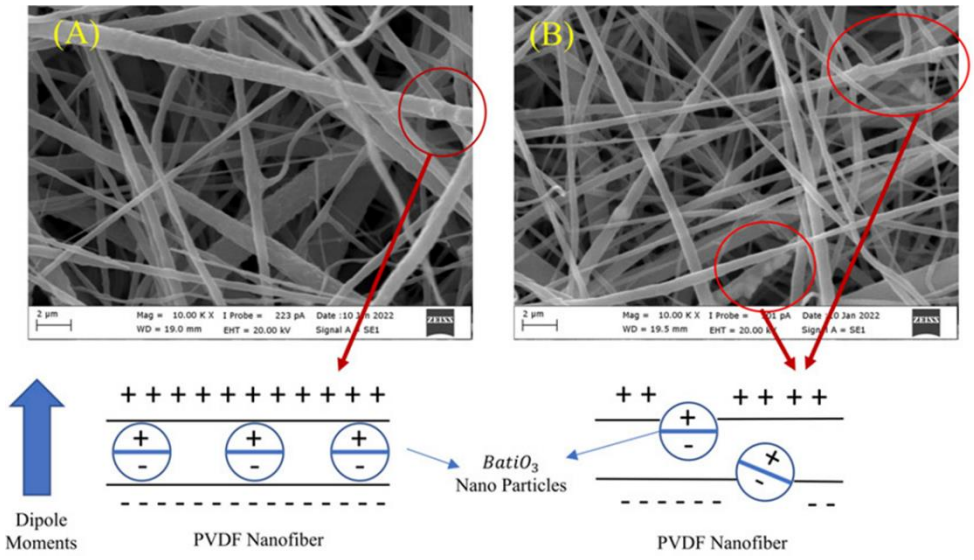

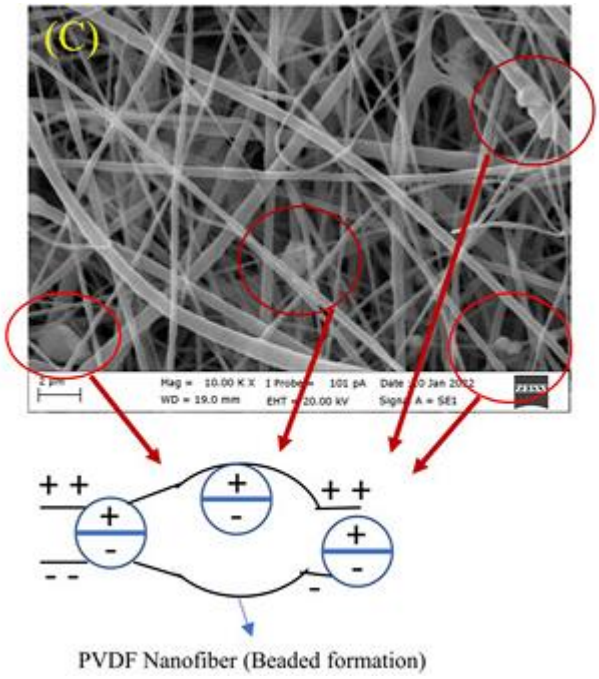

Figure 9: SEM images of electro-spun PVDF/BaTiO3 nanocomposites at 10,000x magnification, (a) PVDF/5%BaTiO3, (b) PVDF/10%BaTiO3, (c) PVDF/15%BaTiO3.

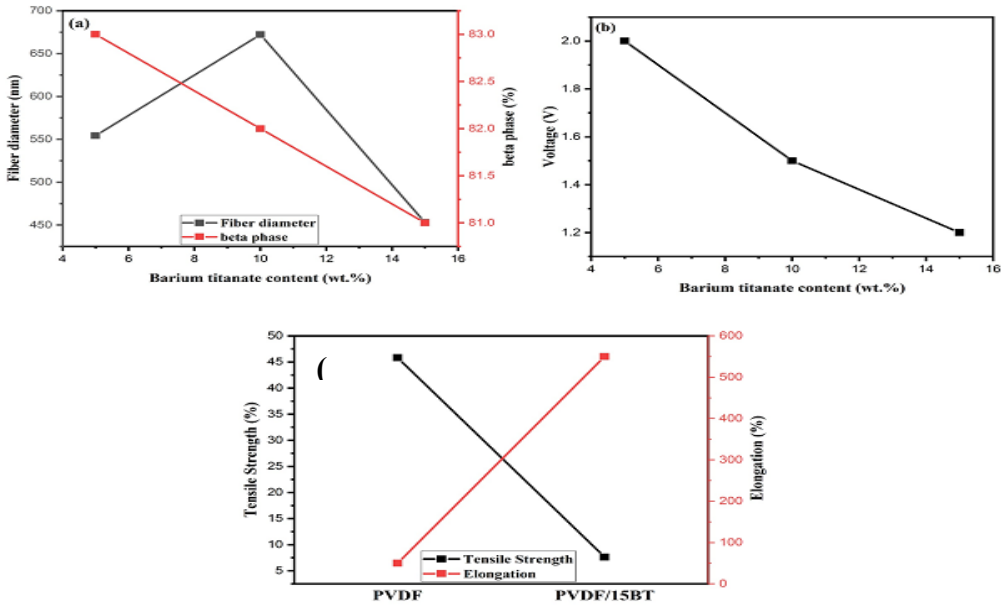

Figure 10: effect Barium titanate and fiber diameter (a) beta phase, (b) voltage outputs, (c) tensile properties.

In 3D Printing, the table shows the samples, including non-poled PVDF and poled PVDF, exhibit varying degrees of β-phase percentages, D33 values (in PC/N), and current measurements (in nA). Non-poled PVDF starts with a β-phase of 42.87, a D33 value of 0.007, and a current of 0.0039. After poling, PVDF shows an increase in β-phase (44.87) and higher D33 (0.010) and current (0.0065). The addition of Barium Titanate (BT) in concentrations from 3% to 15% leads to a progressive increase in β-phase, D33, and current values. Notably, the table succinctly captures the impact of poling and Barium Titanate content on the structural and electrical properties of the PVDF composites

Table: Comparison of β-phase, D33 (Piezoelectric Coefficient), and Current Output for Various PVDF-Based Samples [67]

Sample	β-phase	D33 (PC/N)	Current (nA)
Non-poled PVDF	**42.87**	**0.007**	**0.0039**
Poled PVDF	**44.87**	**0.010**	**0.0065**
PVDF/3%BT	**45.41**	**0.013**	**0.0073**
PVDF/6%BT	**46.73**	**0.029**	**0.0075**
PVDF/9%BT	**51.18**	**0.055**	**0.0168**
PVDF/12%BT	**53.25**	**0.07**	**0.0294**
PVDF/15%BT	**55.91**	**0.101**	**0.0442**

Furthermore, in order to explore the influence of processing on crystallization, Figure 11 depicts the outcomes of employing high-energy ball cryo-milling on PVDF, coupled with blending processes featuring various concentrations of barium titanate. This investigation aims to examine the effects of these processing techniques on the crystallinity and beta phase characteristics observed in different PVDF films. The PVDF film exhibited 13 improvement in crystallinity and 0.38 beta phase, while the milled film showed slightly higher values at 19 and 0.45, respectively. Films with Barium Titanate (BT) additions (ranging from 1% to 10%) displayed diverse crystallinity and beta phase outcomes. For instance, PVDF/1BT showed 19% improvements crystallinity and 0.49% beta phase, PVDF/5BT exhibited 19.3 improvements crystallinity and 0.57 % beta phase, and PVDF/10BT recorded the highest crystallinity at 23.2 with a beta phase of 0.59 (as indicated in Figure 11(b), depicting the evolution of absorbance for the a-phase band centered at 762 cm-1 with temperature and its effect on beta phase content). These findings underscore the influence of BT concentration on PVDF film properties, revealing an increasing trend with higher BT content [68]

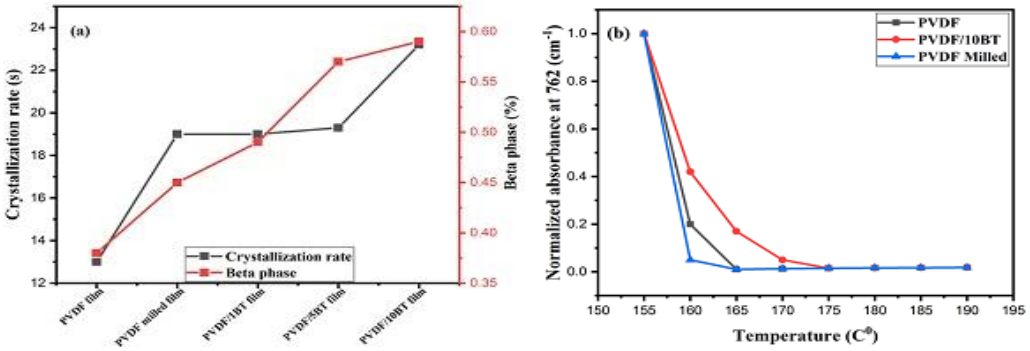

Figure 11. A) Relative crystallization rate depend on type of sample, b) Evolution with temperature of the absorbance for the a-phase band centered at 762 cm^{-1} .

Figure 13 presents Atomic Force Microscopy (AFM) images depicting the topography of cryo-milled PVDF films with varying contents of Barium Titanate (BT) particles (0%, 1%, 5%, and 10%). The images reveal that the inclusion of BT particles within the polymer results in a higher number of smaller spherulites, suggesting increased nucleation due to the milling effect of the particles. This observation aligns with findings from Differential Scanning Calorimetry (DSC) and Fourier-Transform Infrared Attenuated Total Reflection (FTIR-ATR) analyses. Furthermore, at higher magnification, changes in the lamellar aspect ratio are evident with varying BT particle concentrations. In the absence of BT, lamellas appear shorter with an average thickness of 29 nm. Conversely, a greater amount of BT leads to longer and thicker lamellas, approximately 35 nm. Although these morphological changes do not imply alterations in crystalline phases, as indicated by FTIR and XRD results, they are likely to influence macroscopic properties crucial for final applications.

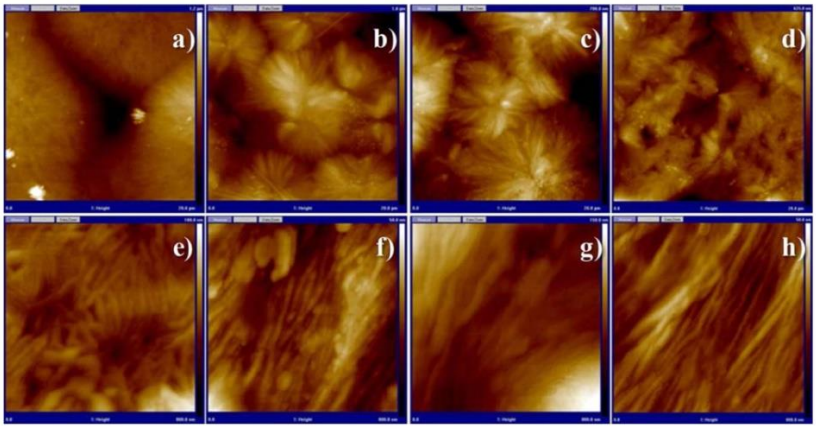

FIG. 12. AFM images of the topography of cryomilled PVDF in the form of films with different contents of BT nanoparticles: (a and e) 0%; (b and f) 1%; (c and g) 5%; and (d and h) 10%. Top images 20 mm 3 20 mm and bottom images 800 nm 3 800 nm.

CONCLUSION

In summary, this study has extensively examined the crystal growth and characterization of PVDF/Barium Titanate (BT) nanocomposites, specifically focusing on the impact of diverse processing techniques, such as 3D printing, electrospinning, and compression molding, on the crystallinity and beta phase. Through the use of analytical tools like X-ray Diffraction (XRD), Fourier-Transform Infrared Spectroscopy (FTIR), and Scanning Electron Microscopy (SEM), the study has provided nuanced insights into the structural changes and molecular interactions within the nanocomposites. The systematic exploration of BT addition's effects on dielectric and piezoelectric properties, considering parameters like particle size, barium titanium content, and shape during manufacturing, has revealed substantial improvements in polyvinyl fluoride crystallization and beta-phase development. The study contributed to understanding the correlation between increased crystallization and enhanced properties of the PVDF/BT nanocomposite. Consequently, future studies can focus on optimizing crystallization and integrating manufacturing methods to achieve the desired quality in applications.

REFERENCES

[1] Arka, Chatterjee, Avijit Das, Kundan Saha, Unyong Jeong. "Nanofiller-Induced Enhancement of PVDF Electroactivity for Improved Sensing Performance." Advanced Sensor Research, vol. 2, 2023. doi: 10.1002/adsr.202200080.

[2] Mengdi Zhang, Cheng-Kun Liu, Bo-tao Li, Yutong Shen, Hao Wang, Keyu Ji, Xue Mao, Liang Wei, Runjun Sun, Fenglei Zhou. "Electrospun PVDF-based piezoelectric nanofibers: materials, structures, and applications." Nanoscale advances, vol. 5, 2023, pp. 1043-1059. doi: 10.1039/d2na00773h.

[3] Soha Mohammadpourfazeli, Shabnam Arash, Afshin Ansari, Shengyuan Yang, Kaushik Mallick, Roohollah Bagherzadeh. "Future prospects and recent developments of polyvinylidene fluoride (PVDF) piezoelectric polymer; fabrication methods, structure, and electro-mechanical properties." RSC Advances, vol. 13, 2022, pp. 370-387. doi: 10.1039/d2ra06774a.

[4] Ram Jeewan Sengwa, Naresh Kumar, Mukul Saraswat. "Morphological, structural, optical, broadband frequency range dielectric and electrical properties of PVDF/PMMA/BaTiO3 nanocomposites for futuristic microelectronic and optoelectronic technologies." Materials today communications, vol. 35, 2023, p. 105625. doi: 10.1016/j.mtcomm.2023.105625.

[5] Kun Liu, Haijun Wang, Yao Wu, Yongxiang Wang, Chun Hua Yuan. "Preparation and properties of gamma-PVDF/lead zirconium titanate composites." Polymer, vol. 281, 2023, p. 126091. doi: 10.1016/j.polymer.2023.126091.

[6] Robertas Grigalaitis, R. Šalaševičius, Juras Banys, M.M. Vijatović Petrović, A.S. Dzunuzovic, M. Ap, Zaghete, Guilhermina Ferreira Teixeira, B.D. Stojanovic.

"Functional properties of PVDF-based NZF-BT flexible films." Lithuanian Journal of Physics, vol. 62, 2022. doi: 10.3952/physics.v62i4.4825.

[7] Shaojing Wang, Peng Xu, Xiangyi Xu, Da Kang, Jie Chen, Zhe Li, Xingyi Huang. "Tailoring the Electrical Energy Storage Capability of Dielectric Polymer Nanocomposites via Engineering of the Host–Guest Interface by Phosphonic Acids." Molecules, vol. 27, 2022, p. 7225. doi: 10.3390/molecules27217225.

[8] Cui Zhaoliang et al. "Crystalline polymorphism in poly (vinylidenefluoride) membranes." Progress in Polymer Science, vol. 51, 2015, pp. 94-126.

[9] Chu Zhaozhe et al. "Effects of strain rate and temperature on polymorphism in flow-induced crystallization of Poly (vinylidene fluoride)." Polymer, vol. 203, 2020, p. 122773.

[10] Lin Taotao et al. "Effect of PMMA molecular weight on its localization during crystallization of PVDF in their blends." Polymers, vol. 13, no. 23, 2021, p. 4138.

[11] Yang Jiao, Benjamin J. McCoy, Giridhar Madras. "A distribution kinetics approach for crystallization of polymer blends." The Journal of Physical Chemistry B, vol. 110, no. 31, 2006, pp. 15198-15204.

[12] Sheth J, Kumar D, Tiwari VK, Maiti P. "Silicon carbide-induced piezoelectric β-phase in poly (vinylidene fluoride) and its properties." J Mater Res, vol. 27, no. 14, 2012, pp. 1838-1845. doi: 10.1557/jmr.2012.133.

[13] Wang Q, Jiang S, Zhang Y, Zhang G, Xiong L. "Microstructure and morphology in the PVDF films doped with BiCl3." Polymer Bull, 2011;66:821-830. doi: 10.1007/s00289-011-0533-z.

[14] Gonçalves R, Lopes AC, Botelho G, Neves IC, Lanceros-Mendez S. "Influence of solvent properties on the electrical response of poly (vinylidene fluoride)/NaY composites." J Polym Res, 2013;20:1-8. doi: 10.1007/s10965-012-0056-7.

[15] Patro TU, Mhalgi MV, Khakhar DV, Misra A. "Studies on poly (vinylidene fluoride)–clay nanocomposites: effect of different clay modifiers." Polymer, vol. 49, no. 16, 2008, pp. 3486-3499. doi: 10.1016/j.polymer.2008.05.035.

[16] Kim JW, Cho WJ, Ha CS. "Morphology, crystalline structure, and properties of poly (vinylidene fluoride)/silica hybrid composites." J Polym Sci B Polym Phys, vol. 40, no. 1, 2002, pp. 19-30. doi: 10.1002/polb.10065.

[17] Xiujuan Lin, Feng Yu, Xiaofang Zhang, Wenlong Li, Yaoting Zhao, Xuan Fei, Qi Jin Li, C. Yang, Shifeng Huang. "Wearable Piezoelectric Films Based on MWCNT-BaTiO3/PVDF Composites for Energy Harvesting, Sensing, and Localization." ACS Applied Nano Materials. doi: 10.1021/acsanm.3c01792.

[18] Caifeng Chen, Feixiang Cai, Yuan Zhu, Linchen Liao, Jilong Qian, Fuh-Gwo Yuan, Ningyi Zhang. "3D printing of electroactive PVDF thin films with high β-phase content." Smart Materials and Structures, vol. 28, no. 6, 2019, p. 065017. doi: 10.1088/1361-665X/AB15B7.

[19] Seong Hyeok Choi, Yoon Seok Lee, Sang Heun Lee, Kyu-Ha Beak, Seungchan Cho, Ilguk Jo, Yangdo Kim, Kyoung-Seok Moon, Moon Hee Choi. "Enhancement of dielectric properties and microstructure control of BaTiO3 by seed-induced solid-state synthesis." Ceramics International, vol. 49, 2023, pp. 17921-17929. doi: 10.1016/j.ceramint.2023.02.159.

[20] V. Sherlin Vinita, Sajeeka Jeyakumar, C. S. Biju. "Sol-gel synthesis, structural, morphological, X-ray photoelectron spectroscopy and magnetic properties of Cd doped BaTiO3 nanostructures." Molecular Crystals and Liquid Crystals, 2023, pp. 1-9. doi: 10.1080/15421406.2023.2228644.

[21] X. Chen et al. "Hydrothermal synthesis of barium titanate nanoparticles and their photocatalytic activity." Journal of Colloid and Interface Science, 2008.

[22] Joan Josep Suñol, L. Escoda. "Novel Materials Synthesis by Mechanical Alloying/Milling." Materials, vol. 15, 2022, p. 6973. doi: 10.3390/ma15196973.

[23] Sonia Kudłacik-Kramarczyk, Anna Drabczyk, Magdalena Głąb, Piotr Dulian, Rafał Bogucki, Krzysztof Miernik, Agnieszka Sobczak-Kupiec, Bożena Tyliszczak. "Mechanochemical Synthesis of BaTiO3 Powders and Evaluation of Their Acrylic Dispersions." Materials, vol. 13, 2020. doi: 10.3390/MA13153275.

[24] Haoyu Qian, Guisheng Zhu, Huarui Xu, Xiuyun Zhang, Yunyun Zhao, Dongliang Yan, Xianyong Hong, Yin Han, Fu Zhenxiao, Ta Shiwo, Aibing Yu. "Preparation of tetragonal barium titanate nanopowders by microwave solid-state synthesis." Applied Physics A, vol. 126, 2020. doi: 10.1007/S00339-020-03472-Y.

[25] Alessandro Dell'Era, Michelina Catauro. "Sol–Gel Method Applied to Crystalline Materials." 2021, p. 903. doi: 10.3390/CRYST11080903.

[26] Ting Wang, Xiaoxiao Pang, Bin Liu, Jie Liu, Jing Shen, Cheng Zhong. "A Facile and Eco-Friendly Hydrothermal Synthesis of High Tetragonal Barium Titanate with Uniform and Controllable Particle Size." Materials, vol. 16, 2023. doi: 10.3390/ma16114191.

[27] Fernando Pereira de Sá, Mariana R.F. Silva, Maxim V. Ivanov, Alexander Tkach, Paula M. Vilarinho, Paula Ferreira. "Hydrothermal Synthesis of Barium Titanate Nanoparticles: The Effect of the Heating System." 2022. doi: 10.3390/materproc2022008141.

[28] "Structural Characterization of Europium-Doped BaTiO3 Obtained by Solid-State Reaction Synthesis." 2022, pp. 553-559. doi: 10.1007/978-3-031-22576-5_56.

[29] S. V. Egorov, A. G. Eremeev, V. V. Kholoptsev, I. V. Plotnikov, Kirill I. Rybakov, Andrey A. Sorokin, Stanislav Balabanov, Elena Ye. Rostokina. "Rapid sintering of barium titanate ceramics using direct and susceptor-assisted microwave heating." Materialia, vol. 24, 2022, p. 101513. doi: 10.1016/j.mtla.2022.101513.

[30] Biljana Stojanović, Biljana Stojanović, Alexandre Zirpoli Simões, Carlos O. Paiva-Santos, Čedomir Jovalekić, Vojislav V. Mitić, José Arana Varela. "Mechanochemical synthesis of barium titanate." Journal of The European Ceramic

Society, vol. 25, 2004, pp. 1985-1989. doi: 10.1016/J.JEURCERAMSOC.2005.03.003.

[31] Rohan Sagar, Mulayam Singh Gaur, Alexandr A. Rogachev. "Piezoelectric and pyroelectric properties of ceramic nanoparticles-based nanostructured PVDF/PVC blend nanocomposites." Journal of Thermal Analysis and Calorimetry, vol. 146, no. 2, 2021, pp. 1-11. doi: 10.1007/S10973-020-09979-Z.

[32] Chanmal C. V., Jog J. P. "Dielectric relaxations in PVDF/BaTiO3 nanocomposites." Express Polymer Letters, vol. 2, no. 4, 2008, pp. 294-301.

[33] Shangyuan Yang, Zhao Xin Zhang, Ai-Ping Zhang, Hai Lan Lin, Xun Zhang, Liuqing Xiao, Jun Bian, Daiqiang Chen. "Preparation and properties of polyimide dielectric nanocomposites containing polyvinylpyrrolidone chemically functionalized barium titanate by in-situ synthesis compounding." Journal of Applied Polymer Science, vol. 139, 2022. doi: 10.1002/app.53231.

[34] Xie X., He Z. Z., Qi X. D., Yang J. H., Lei Y. Z., Wang Y. "Achieving high performance poly (vinylidene fluoride) dielectric composites via in situ polymerization of polypyrrole nanoparticles on hydroxylated BaTiO3 particles." Chemical Science, vol. 10, no. 35, 2019, pp. 8224-8235.

[35] Abdul Aabid, Adibah Amir, Muneer Baig. "Advancements and Limitations in 3D Printing Materials and Technologies: A Critical Review." Polymers, 2023. doi: 10.3390/polym15112519.

[36] Shi X., Zhou W., Ma D., Ma Q., Bridges D., Ma Y., Hu A. "Electrospinning of nanofibers and their applications for energy devices." Journal of Nanomaterials, vol. 16, no. 1, 2015, p. 122.

[37] A comprehensive review summarizing the effect of electrospinning parameters and potential applications of nanofibers in biomedical and biotechnology, Arabian Journal of Chemistry, vol. 11, no. 8, 2018, pp. 1165-1188. doi: 10.1016/j.arabjc.2015.11.015.

[38] Åkermo M., Åström B. T. "Modelling component cost in compression moulding of thermoplastic composite and sandwich components." Composites Part A: Applied science and manufacturing, vol. 31, no. 4, 2000, pp. 319-333.

[39] Elisabetta Brunengo, Lucia Conzatti, Ilaria Schizzi, Chiara Costa, Maria Teresa Buscaglia, Giovanna Canu, Maila Castellano, Vincenzo Buscaglia, Paola Stagnaro. "PVDF/BaTiO3 composites as dielectric materials: Influence of processing on properties." 2018. doi: 10.1063/1.5045994.Shiping, Song., Yijun, Li., Qi, Wang., Chuhong, Zhang. "Facile preparation of high loading filled PVDF/BaTiO3 piezoelectric composites for selective laser sintering 3D printing." RSC Advances, 11 (2021).:37923-37931. doi: 10.1039/D1RA06915B.

[40] Mukesh Kumar, Germán Jiménez-Montes, Nikhil Dilip Kulkarni, Poonam Kumari. "Fabrication and characterization of PVDF/BaTiO3 nanocomposite for energy harvesting application." Materials Today: Proceedings, 2021. doi: 10.1016/J.MATPR.2021.11.133.

[41] Dania Olmos, Gustavo González-Gaitano, Andrei L. Kholkin, Javier González-Benito. "Flexible PVDF-BaTiO3 Nanocomposites as Potential Materials for Pressure Sensors." Ferroelectrics, vol. 447, 2013, pp. 9-18. doi: 10.1080/00150193.2013.821834.

[42] G. Kaur, D. S. Rana. "Synthesis and comprehensive study of polyvinylidene fluoride–nickel oxide–barium titanate (PVDF–NiO–BaTiO 3) hybrid nanocomposite films for enhancement of the electroactive beta phase." Journal of Materials Science: Materials in Electronics, vol. 31, 2020, pp. 18464-18476.

[43] Subramaniyan Ramasundaram, Ashiqur Rahaman, Byungki Kim. "Direct preparation of β-crystalline poly(vinylidene fluoride) nanofibers by electrospinning and the use of non-polar silver nanoparticles coated poly(vinylidene fluoride) nanofibers as electrodes for piezoelectric sensor." Polymer, 2019. doi: 10.1016/J.POLYMER.2019.121910.

[44] Wei-Sheng Guan, Han-Xiong Huang, Bin Wang. "Topographic design and application of hierarchical polymer surfaces replicated by microinjection compression molding." Journal of Micromechanics and Microengineering, 2013. doi: 10.1088/0960-1317/23/10/105010.

[45] Ali Payami Golhin, Riccardo Tonello, Jeppe Revall Frisvad, Sotirios Grammatikos, Are Strandlie. "Surface roughness of as-printed polymers: a comprehensive review." The International Journal of Advanced Manufacturing Technology, 2023. doi: 10.1007/s00170-023-11566-z.

[46] Seth D. McCullen, Derrick Stevens, Wesley A. Roberts, Satyajeet Ojha, Laura Clarke, Russell E. Gorga. "Morphological, Electrical, and Mechanical Characterization of Electrospun Nanofiber Mats Containing Multiwalled Carbon Nanotubes." Macromolecules, 2007. doi: 10.1021/MA061735C.

[47] Elisabetta Brunengo, Lucia Conzatti, Ilaria Schizzi, Chiara Costa, Maria Teresa Buscaglia, Giovanna Canu, Maila Castellano, Vincenzo Buscaglia, Paola Stagnaro. "PVDF/BaTiO3 composites as dielectric materials: Influence of processing on properties." 2018. doi: 10.1063/1.5045994.

[48] Xin Hu, Hui Zhang, De Yu Wu, D.P. Yin, Ning Zhu, Kai Guo, Chunhua Lu. "PVDF-based matrix with covalent bonded BaTiO3 nanowires enabled ultrahigh energy density and dielectric properties." Chemical Engineering Journal, vol. 451, 2022, p. 138391. doi: 10.1016/j.cej.2022.138391.

[49] Haixiong Tang, Yirong Lin, Henry A. Sodano. "Synthesis of High Aspect Ratio BaTiO3 Nanowires for High Energy Density Nanocomposite Capacitors." Advanced Energy Materials, vol. 3, no. 4, 2013, pp. 451-456. doi: 10.1002/AENM.201200808.

[50] Kim, H., Torres, F., Villagran, D., Stewart, C., Lin, Y., & Tseng, T. L. B. (2017). "3D printing of BaTiO3/PVDF composites with electric in situ poling for pressure sensor applications." Macromolecular Materials and Engineering, vol. 302, no. 11, 2017, p. 1700229.

[51] Liu, X., Shang, Y., Liu, J., Shao, Z., & Zhang, C. (2022). "3D printing-enabled in-situ orientation of BaTi2O5 nanorods in β-PVDF for high-efficiency piezoelectric energy harvesters." ACS Applied Materials & Interfaces, vol. 14, no. 11, 2022, pp. 13361-13368.

[52] Hang Luo, Xuefan Zhou, Ru Guo, Xi Yuan, Chen Hehao, Isaac Abrahams, Dou Zhang. (2020). "3D printing of anisotropic polymer nanocomposites with aligned BaTiO3 nanowires for enhanced energy density." DOI: 10.1039/D0MA00045K.

[53] Güçlü, H., Kasım, H., & Yazici, M. (2023). "Investigation of the optimum vibration energy harvesting performance of electrospun PVDF/BaTiO3 nanogenerator." Journal of Composite Materials, vol. 57, no. 3, 2023, pp. 409-424.

[54] Shi, K., Chai, B., Zou, H., Shen, P., Sun, B., Jiang, P., ... & Huang, X. (2021). "Interface induced performance enhancement in flexible BaTiO3/PVDF-TrFE based piezoelectric nanogenerators." Nano Energy, vol. 80, 2021, p. 105515.

[55] Avinash Baji, Yiu-Wing Mai. (2018). "Effect of Barium Titanate Reinforcement on Tensile Strength and Dielectric Response of Electrospun Polyvinylidene Fluoride Fibers." DOI: 10.5772/INTECHOPEN.74662.

[56] Kumar, M., Kulkarni, N. D., & Kumari, P. (2022). "Fabrication and characterization of PVDF/BaTiO3 nanocomposite for energy harvesting application." Materials Today: Proceedings, vol. 56, 2022, pp. 1151-1155.

[57] Brunengo, E., Conzatti, L., Schizzi, I., Buscaglia, M. T., Canu, G., Curecheriu, L., ... & Buscaglia, V. (2021). "Improved dielectric properties of poly (vinylidene fluoride)–BaTiO3 composites by solvent-free processing." Journal of Applied Polymer Science, vol. 138, no. 12, 2021, p. 50049.

[58] Mendes, S. F., Costa, C. M., Caparrós, C., Sencadas, V., & Lanceros-Méndez, S. (2012). "Effect of filler size and concentration on the structure and properties of poly (vinylidene fluoride)/BaTiO 3 nanocomposites." Journal of Materials Science, vol. 47, 2012, pp. 1378-1388.

[59] Baji, A., Mai, Y. W., & Lin, T. (2018). "Effect of barium titanate reinforcement on tensile strength and dielectric response of electrospun polyvinylidene fluoride fibers." In Novel Aspects of Nanofibers, IntechOpen.Mokhtari, F., Spinks, G. M., Sayyar, S., & Foroughi, J. (2021). Dynamic mechanical and creep behaviour of meltspun pvdf nanocomposite fibers. Nanomaterials, 11(8), 2153.

[60] Liu, X., Shang, Y., Liu, J., Shao, Z., & Zhang, C. (2022). "3D printing-enabled in-situ orientation of BaTi2O5 nanorods in β-PVDF for high-efficiency piezoelectric energy harvesters." ACS Applied Materials & Interfaces, vol. 14, no. 11, 2022, pp. 13361-13368.

[61] Avinash Baji, Yiu-Wing Mai. (2018). "Effect of Barium Titanate Reinforcement on Tensile Strength and Dielectric Response of Electrospun Polyvinylidene Fluoride Fibers." DOI: 10.5772/INTECHOPEN.74662.

[62] Kim, H., Torres, F., Villagran, D., Stewart, C., Lin, Y., & Tseng, T. L. B. (2017). "3D printing of BaTiO3/PVDF composites with electric in situ poling for pressure sensor applications." Macromolecular Materials and Engineering, vol. 302, no. 11, 2017, p. 1700229.

[63] Goyal, R. K., Namjoshi, A. H., & Joshi, B. B. (2011, November). "Fabrication and properties of PVDF/BaTiO 3 nanocomposites for electronic applications." In International Conference on Nanoscience, Engineering and Technology (ICONSET 2011), IEEE, 2011, pp. 642-645.

[64] Güçlü, H., Kasım, H., & Yazici, M. (2023). "Investigation of the optimum vibration energy harvesting performance of electrospun PVDF/BaTiO3 nanogenerator." Journal of Composite Materials, vol. 57, no. 3, 2023, pp. 409-424.

[65] Goyal, R. K., Namjoshi, A. H., & Joshi, B. B. (2011, November). "Fabrication and properties of PVDF/BaTiO 3 nanocomposites for electronic applications." In International Conference on Nanoscience, Engineering and Technology (ICONSET 2011), IEEE, 2011, pp. 642-645.

[66] Olmos, D., Montero, F., González-Gaitano, G., & González-Benito, J. (2013). "Structure and morphology of composites based on polyvinylidene fluoride filled with BaTiO3 submicrometer particles: Effect of processing and filler content." Polymer composites, vol. 34, no. 12, 2013, pp. 2094-2104.